Environmental Science & Technology

Article

pubs.acs.org/est

Which Molecular Features Affect the Intrinsic Hepatic Clearance Rate of Ionizable Organic Chemicals in Fish?

Yi Chen,[†] Joop L. M. Hermens,[†] Michiel T. O. Jonker,[†] Jon A. Arnot,[‡,§] James M. Armitage,[‡,§] Trevor Brown,[§] John W. Nichols,[∥] Kellie A. Fay,[∥] and Steven T. J. Droge*[,†,¶]

[†]Institute for Risk Assessment Sciences, Utrecht University, Utrecht, 3508 TD, The Netherlands

[‡]Department of Physical and Environmental Sciences, University of Toronto Scarborough, Toronto, Ontario M1C 1A4, Canada

[§]ARC Arnot Research and Consulting, Toronto, Ontario M4M 1W4, Canada

[∥]US Environmental Protection Agency, Office of Research and Development, National Health and Environmental Effects Research Laboratory, Mid-Continent Ecology Division, Duluth, Minnesota 55804, United States

Supporting Information

ABSTRACT: Greater knowledge of biotransformation rates for ionizable organic compounds (IOCs) in fish is required to properly assess the bioaccumulation potential of many environmentally relevant contaminants. In this study, we measured in vitro hepatic clearance rates for 50 IOCs using a pooled batch of liver S9 fractions isolated from rainbow trout (*Oncorhynchus mykiss*). The IOCs included four types of strongly ionized acids (carboxylates, phenolates, sulfonates, and sulfates), three types of strongly ionized bases (primary, secondary, tertiary amines), and a pair of quaternary ammonium compounds (QACs). Included in this test set were several surfactants and a series of beta-blockers. For linear alkyl chain IOC analogues, biotransformation enzymes appeared to act directly on the charged terminal group, with the highest clearance rates for tertiary amines and sulfates and no clearance of QACs. Clearance rates for C_{12}−IOCs were higher than those for C_8−IOC analogues. Several analogue series with multiple alkyl chains, branched alkyl chains, aromatic rings, and nonaromatic rings were evaluated. The likelihood of multiple reaction pathways made it difficult to relate all differences in clearance to specific molecular features the tested IOCs. Future analysis of primary metabolites in the S9 assay is recommended to further elucidate biotransformation pathways for IOCs in fish.

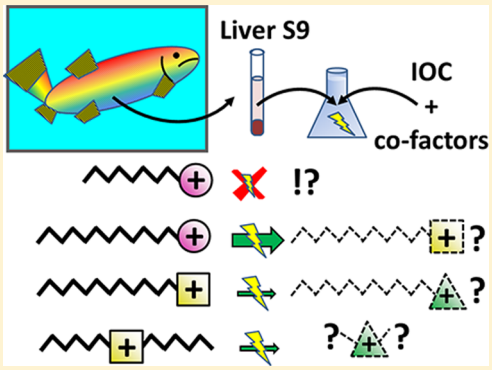

INTRODUCTION

The majority of pharmaceuticals and a substantial percentage of all industrial chemicals are ionizable organic compounds (IOCs).[1−3] A large proportion of these IOCs are acids with a logarithmic dissociation constant (pK_a) < 5 or bases with a pK_a > 8.[1,4] As such, these compounds are predominantly present in their ionic form in aquatic environments and the tissues of exposed organisms. The majority of environmental partitioning and bioaccumulation models have been developed for neutral compounds and neglect the role of pH on the speciation of IOCs and the contribution of ionic species in partitioning processes. Adapting such models to adequately address ionic species requires empirical data and mechanistic insights into all relevant partitioning and reactive processes. Although studies on this topic can be found over the last century,[5−10] the need to better understand the behavior of IOCs has recently received increased attention in the environmental sciences.[11−21]

Combined chemical fate and risk assessment models aim to derive critical exposure concentrations that result in internal concentrations causing adverse effects in exposed organisms.[22−24] The bioconcentration factor (BCF) is a parameter used in hazard and risk assessment of environmental contaminants which links the chemical concentration in water to that in tissues of an exposed organism. A generic BCF prediction model for IOCs in fish (BIONIC V1.0) has been developed, which incorporates partitioning and permeation submodels for neutral and corresponding ionic species.[25] Like other BCF models optimized for neutral compounds,[26−29] the BIONIC-BCF model is based on uptake rates from water and several elimination rates, including those for the processes of branchial elimination, fecal egestion, growth dilution, and biotransformation. For hydrophobic compounds, elimination via biotransformation may result in a measured BCF well below that predicted on the basis of simple equilibrium partitioning.[30−32] The significance of biotransformation as an elimination process for IOCs in fish is less well-known. With the exception of some pharmaceuticals and surfactants,[33−37] the biotransformation of IOCs by fish has rarely been studied.

Received: July 12, 2016
Revised: September 23, 2016
Accepted: October 24, 2016
Published: October 24, 2016

DOI: 10.1021/acs.est.6b03504
Environ. Sci. Technol. 2016, 50, 12722−12731

Table 1. Strongly Acidic Test Compounds with Dissociation Constants (pK_a) and Extrapolated in Vivo Intrinsic Clearance Rates (CL_{int}; mL/h/g liver) Determined from in Vitro Parent Depletion Results Using RT-S9[a]

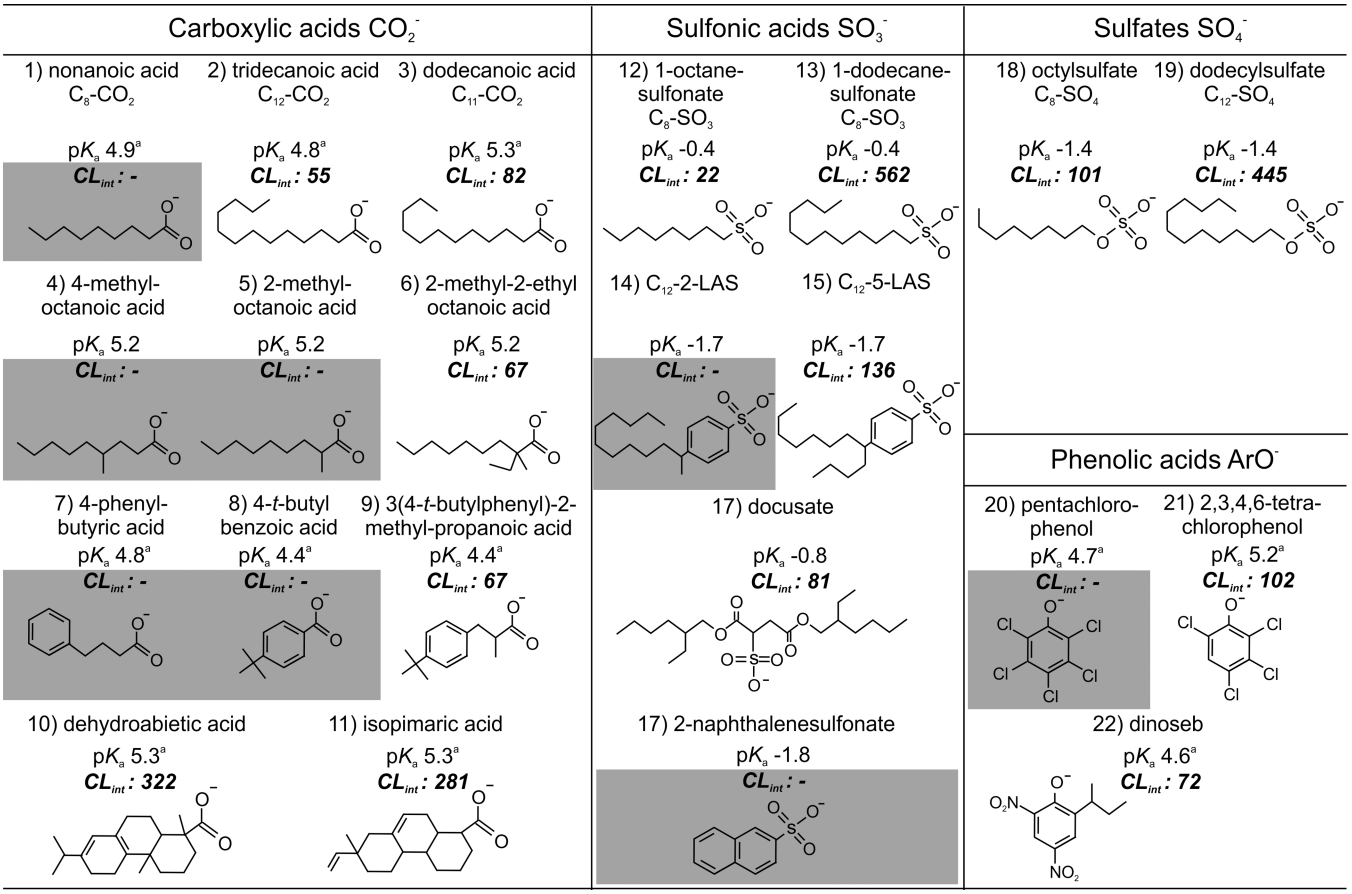

[a]Gray marked IOC structures did not show significant clearance in the RT-S9 assay; all other IOCs showed significant clearance. pK_a values are experimental values (noted with an "a") or estimated with ChemAxon.

On the basis of in vivo testing data with fish, quantitative structure−activity relationships (QSARs) have been constructed for predicting in vivo biotransformation rate constants (k_M) for organic contaminants in fish.[38−41] The experimental data set underlying the development of these k_M−QSARs represents over 600 chemicals, covering a diverse array of structures.[39] However, only 10 of these chemicals are substantially ionized at physiological pH values (>95% ionic at pH 7.4): three bases and seven acids (Section S1, Table S1). A factor complicating the inclusion of more in vivo fish k_M estimates for IOCs relates to the uncertainty in calculating the other uptake and elimination rates. In vitro hepatic clearance assays may provide opportunities to address these uncertainties, because the chemicals are brought in direct contact with enzymes present in fish liver. With adequate in vitro−in vivo extrapolation (IVIVE) modeling,[42] in vitro-based k_M estimates may serve as conservative inputs to BCF models. Moreover, such data could be used as a training set for further development of k_M−QSARs, expanding their current chemical applicability domain.[25,43]

Clearance rates are likely to differ among fish species and tissues[44] and may depend on pre-exposure to other xenobiotics that induce or inhibit specific biotransformation pathways.[45,46] For QSAR development, biotransformation rate data from in vitro assays should be consistent and conservative to capture baseline activity. Liver S9 fractions provide a "complete" metabolizing system, which contains both phase I and phase II biotransformation enzymes.[47] Although S9 fractions have been used to characterize biotransformation rates in several fish species, the rainbow trout (*Oncorhynchus mykiss*) has become a valuable model species, due to the existence of highly standardized assay procedures,[48] as well as important IVIVE parameter estimates.[32] Rainbow trout S9 fractions (RT-S9) were used to study 12 pharmaceuticals that display extensive hepatic metabolism and CYP-isoform selectivity in humans.[47] Eight of these drugs were >90% ionized at the pH of trout plasma (7.8). Of these, significant clearance was measured only for diclofenac (acid, pK_a = 4) and propranolol (base, pK_a = 9.5). On the basis of these results, the metabolic stability of many pharmaceuticals appears to be greater in fish than might be expected on the basis of human clearance data.

The goal of the present study was to measure in vitro fish hepatic clearance rates for 50 IOCs representing the most common types of monoprotic acids and bases. By testing several series of structural analogues, we investigated which basic structural features common to IOCs may determine or influence their metabolic stability in fish. Empirical BCF data are available for 20 of the selected IOCs.[25] The remaining 30 IOCs were selected to populate the series of structural analogues. Included in the entire test set were a number of hydrocarbon-based amines ($C_xH_yN^+$) and a variety of hydrocarbon-based anions ($C_xH_yA^-$). Clearance rates were determined with the RT-S9 assay by measuring rates of parent chemical depletion. In recent years, the "substrate depletion"

DOI: 10.1021/acs.est.6b03504
Environ. Sci. Technol. 2016, 50, 12722−12731

Table 2. Strongly Basic Test Compounds with Dissociation Constants (pK_a) and Extrapolated in Vivo Intrinsic Clearance Rates (CL_{int}; mL/h/g liver) Determined from in Vitro Parent Depletion Results Using RT-S9[a]

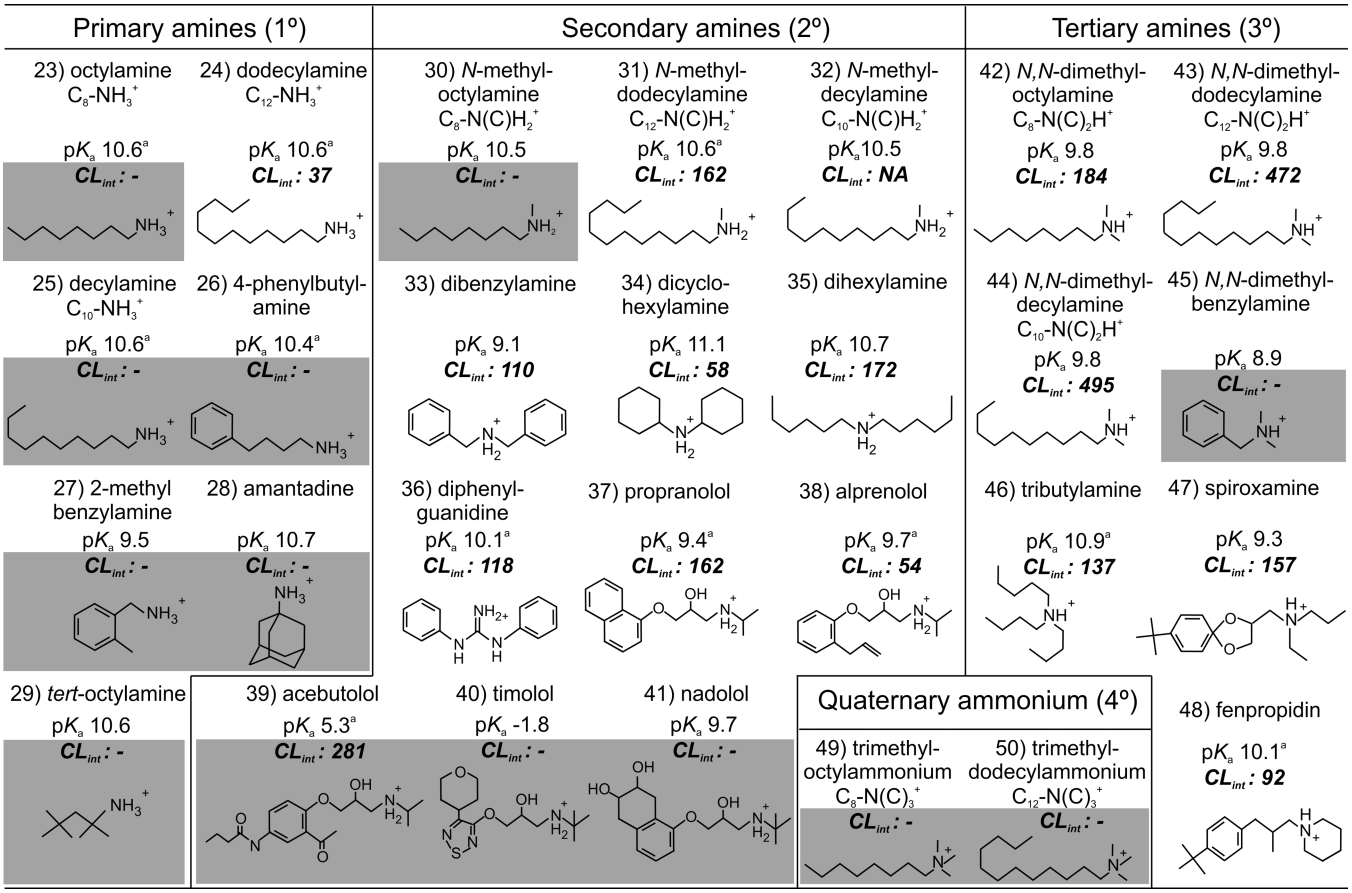

[a]Gray marked IOC structures did not show significant clearance in the RT-S9 assay; all other IOCs showed significant clearance. pK_a values are experimental values (noted with an "a") or estimated with ChemAxon. ‡*N*-Methyldecylamine (#32) was not tested as the parent compound, but it was identified as the most likely 1° metabolite of *N,N*-dimethyldecylamine (Figure 2). NA, not applicable.

approach has gained increasing popularity over the "product formation" approach, as it accounts for all reaction pathways and does not require knowledge of chemical products and their analysis.[32,49−53]

MATERIALS AND METHODS

Brief Outline of the RT-S9 Assay. A detailed description of the RT-S9 assay is provided elsewhere.[48] Specific test conditions are presented in Section S2. The concentration of parent compound spiked into the active S9 matrix was followed over time with duplicates, and each reaction was stopped by the addition of ice-cold acetonitrile. Samples containing heat denatured S9 material were included as a control to account for possible nonenzymatic losses. The main modification of the standard S9 protocol was that for most IOCs we first performed a screening assay with duplicate samples taken at three time points over a 1 or 2 h incubation period. This approach allowed for the testing of three compounds using one sample of active RT-S9, along with a reference base (propranolol) to verify activity. If the depletion curve determined in these experiments did not exhibit a positive slope significantly different from 0, no further tests were performed, saving resources and S9 samples. For chemicals exhibiting significant clearance, additional assays were performed with six time points in studies lasting up to 2 h.

IOCs, Cofactors, and RT-S9 Material. Structures of the 50 IOCs tested are shown in Tables 1 and 2, along with dissociation constants. CAS numbers, suppliers, and purities are presented in Section S3, Table S3. The S9 assays were performed in 100 mM potassium phosphate-buffered saline (PPBS), adjusted to pH 7.8. Stock solutions of the IOCs were prepared as 10 mg/mL in a 20/80 mixture of acetone/PPBS. The nominal starting concentration of each test compound was 0.5 μM. Alamethicin (Sigma-Aldrich, Zwijndrecht, The Netherlands) was added from a methanol stock to support uridine 5′-diphospho-glucuronosyltransferase (UGT) activity.[54] The cofactors nicotinamide adenine dinucleotide 2′-phosphate (NADPH, Sigma-Aldrich), uridine 5′-diphosphoglucuronic acid (UDPGA, Sigma-Aldrich), L-glutathione (GSH, Sigma-Aldrich), and 3′-phosphoadenosine-5′-phosphosulfate (PAPS, Sigma-Aldrich) were added as recommended.[48] All of the IOCs were tested using a single batch of pooled trout liver S9 fractions (active and denatured), prepared by the US EPA in Duluth, MN. The batches had been shipped on dry ice to the testing facilities at Utrecht University. The pooled sample was a composite of material from 5 juvenile males, weighing 453 ± 50 g. Characterization data for this pooled sample is provided in Section S2. Measured levels of ethoxyresorufin-*O*-deethylase (EROD), UGT, and glutathione-*S*-transferase (GST) activity were similar to those reported for other RT-S9 batches originating from the same laboratory.[47,53] Protein concentration

DOI: 10.1021/acs.est.6b03504
Environ. Sci. Technol. 2016, 50, 12722−12731

was determined using Peterson's modification of the micro Lowry assay (Sigma technical bulletin TP0300; Sigma-Aldrich). The S9 suspensions were stored at −80 °C and thawed on ice before use.

Analysis. IOC concentrations in all extracts were quantified with a PerkinElmer liquid chromatography system, coupled to a triple quadrupole/linear ion trap mass spectrometer (API 3000 LC-MS/MS, AB Sciex). Analytical details are presented in Section S2. Subsequently, $\log_{10}$-transformed concentrations (μM) of the parent chemicals were plotted as a function of time (min). The linear portions of the resulting curves, generally encompassing most of the data, were fitted with a linear regression. A first-order depletion rate constant (k_e; h^{-1}) was calculated by multiplying the fitted slope term by −2.3 (i.e., −ln(10)) and then by 60 (to convert from min to h). The in vitro intrinsic clearance rate ($CL_{int,S9\text{-}hep}$; mL/h/mg S9 protein) was calculated by dividing k_e by the S9 protein concentration in the assay. The $CL_{int,S9\text{-}hep}$ was then multiplied by a scaling factor (163 mg S9 protein/g liver) determined previously for *O. mykiss*[32] to estimate an in vivo intrinsic clearance value for liver tissue ($CL_{int,in\ vivo\text{-}hep}$; mL/h/g liver).

RESULTS AND DISCUSSION

General Performance of the RT-S9 Assay. For all tested IOCs, a constant concentration close to the nominal value was measured in heat-inactivated controls (see raw data plots in Section S5), indicating that there were no significant non-enzymatic loss processes and that the recoveries of the acetonitrile extraction procedure were good. The data generated by repeated use of the reference base propranolol showed that there was no loss of RT-S9 activity in stored samples over time and that assays performed using a single batch of RT-S9 can be conducted with a high degree of consistency (Section S4, Figure S1). Figure S2 shows the close correspondence between clearance data obtained in screening experiments and full time-course studies for 12 of the tested IOCs. Out of the 50 compounds tested, no depletion was observed in the screening series for 22 IOCs. The assays for these chemicals were run for 100 min, except for 2-naphthalenesulfonate, octylamine, *N*-methyloctylamine, *N,N*-dimethyloctylamine, and trimethyloctylammonium bromide, which were incubated for 60 min. Incubation for longer than 2 h was not pursued, because the activity of the S9 system has been shown to decline over time.[48]

The ability to detect significant depletion in the S9 assay depends on the reproducibility of the replicates, the total number of time points, and the trend (i.e., fitted slope) over the course of an experiment for both active samples and negative controls. For example, the slope of the linear depletion curve for the quaternary ammonium compound (QAC) trimethyldodecylammonium bromide (IOC #50) was not significantly different from 0 (p = 0.054), although the average concentration in active S9 samples at the last time point was 0.14 log units lower than that in heat inactivated controls. In another experiment, the slope of the depletion curve for 1-octanesulfonate (#12) was significantly different from 0 (p = 0.003) and the average concentration at the last time point was 0.1 log units lower than the average initial concentration, but the slope of the curve was not significantly different from that for the heat-inactivated controls.

The average absolute difference between duplicate values from all experiments was 11 ± 9% and did not exceed 20% (see discussion Section S5, Table S4). Differences between replicates may be caused by variability of the analytical results, heterogeneity of the S9 samples, or experimental variability (e.g., pipetting reproducibility). Simulated depletion curves indicate that, if duplicate values at all 6 time points differ by less than 15%, a decrease in signal of 0.1 log units (down to 80% of the starting concentration) over 100 min is required to achieve a significant difference in slope between active samples and inactive controls (assuming no loss of chemical from controls; p < 0.02) (Section S4, Figure S3). This "lower limit boundary" is case-specific but, in the simulated example, would result in a slope of −0.001 min^{-1}, a k_e of 0.14 h^{-1}, and a $CL_{int,in\ vivo\text{-}hep}$ of 22.5 mL/h/g liver. As shown in Table 1, clearance rates determined for amantadine (#28) and 1-octanesulfonate (#12) were significant but are near this lower limit. These $CL_{int,in\ vivo\text{-}hep}$ values are therefore considered less certain.

IOCs with Significant RT-S9 Clearance. Out of the 50 compounds tested, 28 showed significant (p < 0.05) depletion. For most IOCs, the reaction followed first order kinetics, as illustrated by the reference base propranolol (Figure S1) and the many examples in Figure 1. In contrast, for some IOCs, rapid depletion was observed initially, which then slowed after the first hour (e.g., some C_{12}−IOCs in Figure 1 and others in Section S5). The cause of this apparent second order behavior probably relates to loss of enzymatic activity, for which possible explanations include depletion of required cofactors and product inhibition. For the chemicals concerned, we fitted parent depletion curves to data from the first hour of the incubation, in order to be able to report first order depletion. The resulting data are listed in Table S4. $CL_{int,in\ vivo\text{-}hep}$ values are listed in Table 1 for acids and Table 2 for bases.

RT-S9 Clearance for IOCs with a Single Hydrocarbon Chain. The different IOCs with octyl-chains (C_8) and dodecyl-chains (C_{12}) provided a particularly good opportunity to study the influence of molecular structure on the clearance capacity of RT-S9 (see Figure 1A,B). For the set of seven C_8−IOCs, clearance by RT-S9 was significant only for the tertiary (3°) amine C_8−$N(C)_2H^+$ (#42) and sulfate C_8−SO_4^- (#18) compounds. The fact that five C_8−IOCs were not cleared by RT-S9 suggests that the linear octyl chain is not a target for biotransformation. Instead, the in vitro clearance of C_8−$N(C)_2H^+$ (184 mL/h/g liver) and C_8−SO_4^- (101 mL/h/g liver) was probably caused by enzymes that are specific for these charged functional groups.

In contrast to the C_8−IOCs, significant clearance rates were observed for all C_{12}−IOCs, with the exception of the QAC trimethyldodecylammonium bromide (#50). The absence of clearance for this QAC again suggests the absence of enzymatic activity directed toward the alkyl chain. Clearance rates for the 3° amine C_{12}−$N(C)_2H^+$ (#43), the sulfonate C_{12}−SO_3^- (#13), and the sulfate C_{12}−SO_4^- (#19) were maximal during the first hour but declined thereafter. The initial $CL_{int,in\ vivo\text{-}hep}$ values for these compounds were 472, 455, and 562 mL/h/g liver, respectively. The 2° amine C_{12}−$N(C)H_2^+$ (#31) exhibited log−linear depletion during the full 100 min incubation period (162 mL/h/g liver). Intrinsic clearance rates for the 1° amine C_{12}−NH_3^+ (#24) and carboxylic acid C_{12}−CO_2^- (#2) were significant (37 and 82 mL/h/g liver, respectively) but about a factor of 10 lower than those for the three most rapidly cleared C_{12}−IOCs.

We did not test IOCs with alkyl chains longer than C_{12}, but other IOCs with intermediate linear alkyl chain lengths included decylamine (#25, C_{10}−NH_3^+), *N,N*-dimethyldecylamine (#44, C_{10}−$N(C)_2H^+$), and dodecanoic acid (#3, C_{11}−

DOI: 10.1021/acs.est.6b03504
Environ. Sci. Technol. 2016, 50, 12722−12731

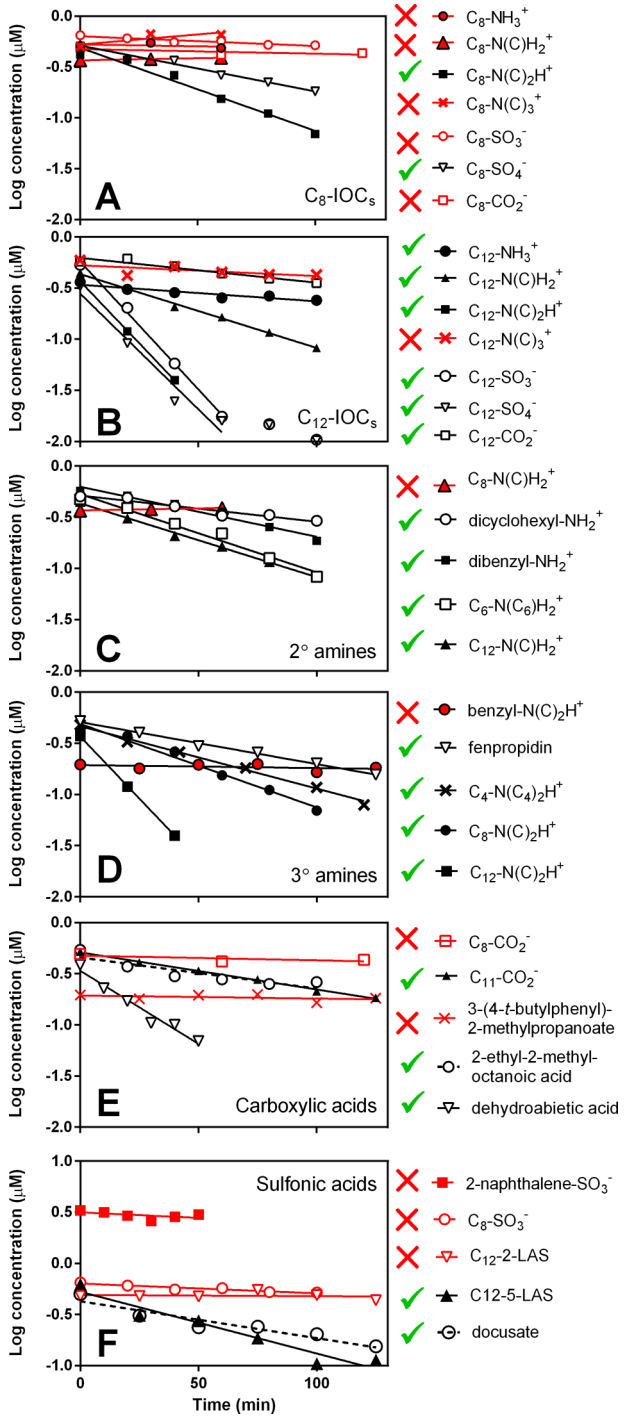

Figure 1. Rainbow trout S9 depletion data and fitted curves for: (A) octylchain-based IOCs; (B) dodecylchain-based IOCs; (C) hydrocarbon-based ($C_xH_yN^+$) 2° amines; (D) hydrocarbon-based ($C_xH_yN^+$) 3° amines; (E) hydrocarbon-based anions ($C_xH_yA^-$), all carboxylic acids; (F) various sulfonates. Duplicate averages are shown; full duplicate data are in Section S5. A red X indicates compounds that were not significantly cleared. A green checkmark indicates compounds that exhibited significant clearance.

CO_2^-). As shown in Table 2, the 1° amine C_{10}–NH_3^+ was not cleared, whereas C_{12}–NH_3^+ showed minimal clearance. The $CL_{int,in\ vivo\text{-}hep}$ of the 3° amine C_{10}–$N(C)_2H^+$ (495 mL/h/g liver) was three times faster than that of C_8–$N(C)_2H^+$ (#42) and essentially identical to that of C_{12}–$N(C)_2H^+$ (#43). Lower clearance rates were observed for both C_{11}–CO_2^- (#3, 82 mL/h/g liver) and C_{12}–CO_2^- (#2, 55 mL/h/g liver). Collectively, these results suggest that both alkyl chain length and the type of ionizable group can impact metabolic clearance rates.

Although most of the experiments performed in this study were conducted using a substrate depletion approach, for the rapidly cleared 3° amine (#44, C_{10}–$N(C)_2H^+$), we attempted to measure production of the putative metabolite C_{10}–$N(C)H_2^+$ (#32) in order to verify the most likely biotransformation pathway. For many 3° amine drugs, N-dealkylation results in production of a 2° amine analogue. These 2° amines can then be biotransformed to 1° amines.[55−58] Although we could only identify the metabolite C_{10}–$N(C)H_2^+$ by the assumed m/z fragment of 172.4 and did not include calibration standards, Figure 2 shows that a strong and

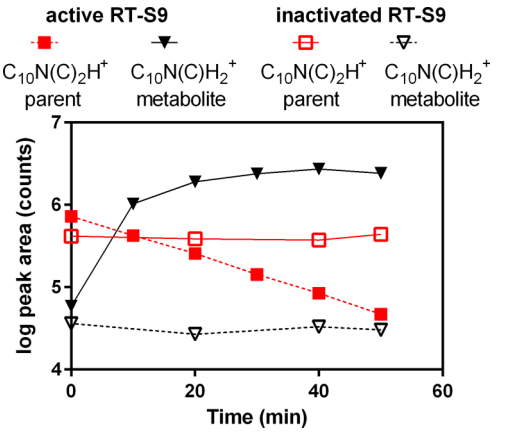

Figure 2. Depletion of the 3° amine C_{10}–$N(C)_2H^+$ and appearance of the 2° amine metabolite C_{10}–$N(C)H_2^+$ in the RT-S9 assay.

increasing metabolite signal was observed during the clearance of C_{10}–$N(C)_2H^+$. This indicates that N-dealkylation is a major transformation process in rainbow trout. Minor traces of apparent C_{10}–$N(C)H_2^+$ were also observed in the assay with heat-inactivated RT-S9 suggesting that C_{10}–$N(C)H_2^+$ was present at low concentrations as an impurity in the original C_{10}–$N(C)_2H^+$ standard. It is likely that other metabolites were formed in the reaction, but optimizing the identification of other metabolites was outside the scope of this study. Future testing of other 2° and 3°amines in the RT-S9 assay could readily incorporate a scan for logical dealkylation products in the LC-MS analysis, confirming the relevance of this biotransformation pathway. However, a lack of standards may still hamper adequate quantification. For structurally complex bases, the larger number of potential phase I and phase II reaction products results in additional analytical challenges, though these could be minimized for pharmaceuticals by collation of biotransformation information for other tested species.[59]

RT-S9 Clearance for Branched $C_xH_yN^+$ IOCs. Whereas the C_8–IOCs and C_{12}–IOCs contain single linear alkyl chains, our test chemical set also included compounds with multiple alkyl chains, branched alkyl chains, aromatic rings, and nonaromatic rings. Figure 1C,D shows depletion curves for different 2° amines and a selection of 3° amines, respectively. Three of the 2° amines have two identical hydrocarbon side chains on the charged nitrogen moiety: dihexylamine, dibenzylamine, and dicyclohexylamine. Dihexylamine (#35, $CL_{int,in\ vivo\text{-}hep}$ 172 mL/h/g liver) was cleared at a similar rate as *N*-methyldodecylamine (#31, 162 mL/h/g liver), which

DOI: 10.1021/acs.est.6b03504
Environ. Sci. Technol. 2016, 50, 12722−12731

contains one additional CH_2 unit. Assuming that the same enzyme in the S9 fraction is transforming these two 2 °$C_xH_yN^+$ amines and that this biotransformation is directed toward the amine group, it appears that the position of the charged nitrogen in both molecular structures is equally accessible. Sorption of the cationic *N*-methyldodecylamine to phospholipids is approximately one-hundred times stronger than that of cationic dihexylamine,[60] suggesting that this "indicator of hydrophobicity" does not correlate with substrate affinity for the enzyme responsible for amine metabolism. Compared to dihexylamine, the intrinsic clearance rates of dibenzylamine (#33) and dicyclohexylamine (#34) were a factor of 1.5 and 3 lower (Table 1; 110 and 58 mL/h/g liver, respectively). The more structurally complex the IOC becomes, the more difficult it is to speculate on the molecular basis for differences in biotransformation rate. The nonaromatic cyclohexyl side groups of dicyclohexylamine may confer lower hydrophobicity to the molecule than the hexyl chains of dihexylamine[60] and could therefore result in lower affinity for the active site of the enzyme; however, steric effects are also possible. For dibenzylamine, it is unlikely that the benzyl groups are targets for biotransformation, since several of the IOCs that were not significantly cleared also contain phenyl rings, such as the 3° amine *N,N*-dimethylbenzylamine (#45) and the sulfonate surfactant C_{12}-2-LAS (#14).

The 3° amine tributylamine (#46) has only one CH_2 unit less than the 3° amine $C_{12}-N(C)_2H^+$ (#43), but the $CL_{int,in\ vivo\text{-}hep}$ (137 mL/h/g liver) was lower than that of $C_{12}-N(C)_2H^+$ (472 mL/h/g liver) and $C_8-N(C)_2H^+$ (#42, 184 mL/h/g liver). This result clearly contrasts with that of the 2° amine pair of dihexylamine (#35) and $C_{12}-N(C)H_2^+$ (#31) and suggests that the presence of all butyl chains on the charged nitrogen results in a lower biotransformation rate than that observed for *N,N*-dimethyl(C_xH_y)amine compounds. Fenpropidin (#48) contains an ionizable nitrogen atom as part of a nonaromatic ring and is metabolized at a relatively low (92 mL/h/g liver), yet measurable, rate. The *tert*-butylphenyl-2-methylpropanoic side group of fenpropidin is also present in the carboxylic acid 3-(4-*tert*-butylphenyl)-2-methylpropanoic acid (#9), which did not exhibit measurable biotransformation. This finding indicates that there are no significant enzymatic reactions directed toward this branched side chain and suggests instead that fenpropidin is transformed mainly at the (charged) piperidine ring.

RT-S9 Clearance for Branched $C_xH_yA^-$ IOCs. Three carboxylic acids with a branched group next to the charged $C(O)O^-$ unit were not biotransformed by RT-S9:2-methyl-octanoic acid (#5), 4-*tert*-butylbenzoic acid (# 8), and 3-(4-*tert*-butylphenyl)-2-methyl-propanoic acid (#9) (Table 1). Interestingly, 2-ethyl-2-methyl-octanoic acid (#6) exhibited a clear depletion curve (Figure 1E). This suggests that steric hindrance was not the reason for the absence of enzymatic conversion of the three above-mentioned carboxylic acids. The two resin acids dehydroabietic acid (#10) and isopimaric acid (#11) were cleared four times faster (322 and 281 mL/h/g liver, respectively) than the linear chain carboxylic acid $C_{12}-CO_2^-$ (82 mL/h/g liver). It is not clear, however, whether this activity was directed toward the carboxylate unit (as is most likely for $C_{12}-CO_2^-$) or the polycyclic structure. C_{12}-2-LAS (#14) was not cleared, while the isomer C_{12}-5-LAS (#15) showed an intermediate $CL_{int,in\ vivo\text{-}hep}$ of 136 mL/h/g liver (Figure 1F). This finding contrasts with the rapid clearance of the linear $C_{12}-SO_3^-$ and suggests that reactions involving the sulfonate group strongly depend on surrounding molecular features. The higher activity for the inner LAS isomer C_{12}-5-LAS is also inconsistent with the lower clearance rates observed for centrally charged dihexylamine compared to terminally charged $C_{12}-N(C)H_2^+$, indicating that structural trends observed for one IOC type do not necessarily apply to another.

RT-S9 Clearance for IOCs with Multiple Functional Groups. Results obtained for the series of hydrocarbon-based cations ($C_xH_yN^+$) and anions ($C_xH_yA^-$) suggest that enzymatic conversions are largely focused on the charged functional group. However, several of the IOCs contain additional structural features (Tables 1 and 2) that may be targets for enzymatic action. For example, the sulfonate anion docusate (#16) contains two ester groups that are candidates for enzymatic cleavage. Docusate, with a centrally positioned sulfonic group, is cleared by RT-S9, but the clearance rate for this relatively large and branched anion (81 mL/h/g liver) is much lower than that for linear $C_{12}-SO_3^-$ (562 mL/h/g liver) and somewhat lower than that of C_{12}-5-LAS (136 mL/h/g liver, Figure 1). As for LAS, the surrounding molecular features may substantially limit reactions involving the sulfonate group. The hydrophilicity of the structure may also lower its affinity for enzymes that catalyze this activity. Although the intrinsic clearance rate is a useful measure for further studies of docusate, it remains unclear whether the ester groups contribute to its biotransformation.

A careful identification of primary metabolites would provide additional insight into the factors that determine relative S9 clearance rates for a specific molecular feature. For example, depletion data were obtained for a series of five 2° amine beta-blockers (#37−41: propranolol, alprenolol, acebutolol, timolol, and nadolol), four of which share a similar structural backbone with alterations only on the phenyl ring (Table 2). Propranolol (#37) was cleared at an intermediate rate by RT-S9, but acebutolol, timolol, and nadolol were not cleared to any significant extent. The naphthalene structure of propranolol is readily hydroxylated in the liver of rats and humans.[61,62] The only other beta-blocker that was cleared by RT-S9 was alprenolol, which has a vinyl side chain. Alprenolol undergoes N-dealkylation of the isopropyl group in rat liver microsomes, as well as benzylic and aromatic hydroxylation.[63] The primary metabolites of acebutolol in mammals are diacetolol and acetolol. These metabolites, which are excreted in urine, result from enzymatic activity involving the butylamide side chain. However, neither of these metabolites was produced by rat liver microsomes, and it was suggested that these reactions largely occur in nonhepatic tissues.[63] In humans, the primary pathway for metabolism of timolol involves hydroxylation of the morpholine ring.[64] Nadolol undergoes little or no metabolism in mammals and is excreted unchanged in urine.[62] Collectively, these findings suggest that functional groups in the beta-blocker backbone structure, including the secondary amine, may not be major targets for hepatic biotransformation in mammals or fish. Further complicating an evaluation of relative clearance rates for analogous, but multifunctional IOCs, is the fact that some enzymatic processes are enantiomer-specific, as has been observed previously for the metabolism of propranolol by RT-S9[65] and humans.[62] Observed differences in metabolic clearance of different beta-blockers may also partially relate to differences in relative hydrophobicity,[62] as suggested when attempting to explain the lower clearance rates for C_8−IOCs compared to those of C_{12}−IOCs. This may also explain why there was no significant clearance of 2-naphthalenesulfonate

DOI: 10.1021/acs.est.6b03504
Environ. Sci. Technol. 2016, 50, 12722−12731

(#17) which, like propranolol, contains a naphthalene side chain (Figure 1).

Comparisons with Other RT-S9 Studies on IOC Clearance. The increasing in vitro clearance of IOCs with increasing alkyl chain length (single linear chain) agrees to some extent with RT-S9 data and perfused liver clearance rates measured for a series of increasingly hydrophobic polycyclic aromatic hydrocarbons (PAHs).[53] Connors et al.[47] reported a $CL_{int,S9\text{-}hep}$ of 2. 74 mL/h/mg S9 protein for propranolol, which is 2.8 times faster than the value measured in our study. When Connors et al.[47] extrapolated this value to the intact tissue, they used a scaling factor (50 mg S9/g liver) that was based on the microsomal protein content of liver tissue from mammals, while the scaling factor determined specifically for rainbow trout was 163 mg S9/g liver.[32] As a result, the $CL_{int,in\ vivo\text{-}hep}$ value (137 mL/h/g liver) reported by Connors et al.[47] appears close to that determined in the present study (162 mL/h g liver) but was actually a factor of 2.7 higher. Gomez et al.[44] reported a $CL_{int,S9\text{-}hep}$ for propranolol of ∼0.4 mL/h/mg S9 protein (corrected in ref 47), which is a factor of 2.5 lower than that measured in our study. However, Gomez et al.[44] used higher starting concentrations of propanolol (10 μM) than those employed in our study (0.5 μM) and that by Connors et al.[47] In vitro clearance rates are concentration dependent when determined at substrate concentrations close to the Michaelis−Menten affinity constant for the reaction.[66] Tables 1 and 2 list 22 IOCs for which there was no significant clearance. Connors et al.[47] did not observe any clearance for 6 ionized pharmaceuticals. In the present study, there was no measurable depletion of the 2° amine C_8−NH_2^+ and only a moderate clearance for C_{12}−NH_2^+. These observations are consistent with the reported lack of clearance for the 2° amine drugs methylphenidate and fluoxetine in the RT-S9 system.[47] In contrast, the absence of any measurable clearance for the 3° amine diphenhydramine[47] is surprising, given the relatively fast clearance observed in the present study for the other 3° amines.

In a previous study with trout hepatocytes, it was reported that pentachlorophenol undergoes glucuronidation and sulfation of the hydroxyl unit, depleting 40% of the parent compound within 2 h.[33] We did not observe any clearance of this compound (#20) in the RT-S9 assay. In contrast, the phenols dinoseb (#22) and 2,3,4,6-tetrachlorophenol (#21) exhibited measurable clearance. Pentachlorophenol has a lower pK_a value than 2,3,4,6-tetrachlorophenol (4.7 vs 5.6), which results in a lower neutral fraction at the tested pH of 7.8. In either case, however, more than 99% of the test compound was present as the dissociated phenolate anion. For these and other tested compounds, it is unclear to what extent the neutral and ionized forms contributed to observed clearance rates.

Another surprising result was the apparent lack of clearance for C_{12}-2-LAS (#14). Tolls et al.[35] reported that fathead minnows metabolize C_{12}-2-LAS, resulting in estimated k_M's ranging from 0.3 to 0.7 d^{-1}.[35] This in vivo k_M accounted for more than 40% of total elimination in these fish and significantly decreased the measured BCF.[35] On the basis of the observed metabolites, the initial biotransformation process for C_{12}-2-LAS was shown to be ω-oxidation of the alkyl-terminus, followed by a sequence of β-oxidation steps.[35] Using this and other information from fathead minnows,[35,67] Arnot et al.[39] deduced in vivo biotransformation rate constants (k_M) of 0.32 and 0.58 d^{-1} for C_{12}-2-LAS and C_{12}-5-LAS (#15) (normalized to a 10 g fish at 15 °C), respectively. Thus, while fathead minnows have been shown to metabolize both compounds, C_{12}-5-LAS appears to be cleared more rapidly than C_{12}-2-LAS. Dyer et al.[68] studied the biotransformation of ^{14}C labeled C_{12}-2-LAS using liver homogenates and microsomes from common carp and rainbow trout, as well as primary carp hepatocytes and hepatocarcinoma cells from desert topminnow. The clearance rates determined for subcellular fractions from carp and trout (roughly equivalent to the S9 fraction) were 0.076 and 0.282 mL/h/mg protein (∼12 and ∼45 mL/h/g liver),[68] respectively, which are close to the clearance rate threshold determined here for RT-S9. In the present study, the absence of any measurable clearance for C_{12}-2-LAS, combined with the lack of clearance for several IOCs with linear alkyl chains (e.g., C_8−NH_3^+, C_8−CO_2^-, and C_8−SO_3^-), suggests that ω-oxidation does not occur in RT-S9. Alternatively, this reaction may be occurring, but the rate of activity is below the detection threshold. This functional limit on the ability of the RT-S9 assay to detect low enzymatic activity may also explain the apparent lack of metabolism for pentachlorophenol.

Outlook for the Use of in Vitro RT-S9 Clearance Rates in Bioaccumulation Assessments for IOCs. There are merits and limitations to any method used to estimate biotransformation rates in fish. Liver S9 fractions may be prepared for any fish which contains a discrete liver tissue. The resulting material retains its activity when frozen and is easy to ship and use. With regard to the RT-S9 assay, scaling factors developed for trout can be employed to extrapolate measured rates of activity to the intact animal. The resulting k_M estimates may be used at a screening level to assess chemicals for their bioaccumulation potential. Alternatively, this information can be compared to measured k_M values for benchmark chemicals (neutral or IOCs) for which reliable estimates of in vivo k_M and steady-state BCF are available.

The current data set is too small to initiate development of a RT-S9 clearance QSAR. Nevertheless, these data suggest several trends with respect to biotransformation of IOCs: (i) within a chemical series, $CL_{int,in\ vivo\text{-}hep}$ tends to be lower for smaller and/or more polar compounds; (ii) the contribution of cationic moieties to $CL_{int,in\ vivo\text{-}hep}$ is in the order: tertiary amine > secondary amine > primary amines > quaternary ammonium; for anionic moieties, it is: sulfate ∼ sulfonate > phenolate > carboxylate; (iii) the molecular structure surrounding the charged moiety influences $CL_{int,in\ vivo\text{-}hep}$: a neighboring phenyl ring (alkylbenzenesulfonate surfactants) or a central positioning of the charged moiety (tributylamine) seems to reduce intrinsic clearance, while branching does not (carboxylic 2-ethyl-2-methyl-octanoic acid).

With the addition of carefully selected chemical structures to the current test set, existing knowledge of chemical biotransformation in fish can be extended for a number of functional groups and molecular conformations. The substrate depletion approach is of high value because it is easy to perform and takes all transformation processes into account. As such, it may be used to evaluate a substantial number of chemicals in a relatively short period of time, thereby providing a means of prioritizing chemicals for additional study. Follow-up studies that involve analysis of primary metabolites can then help elucidate the main biotransformation pathways involved. Although generating a single hepatic clearance rate QSAR for rainbow trout based on molecular fragments is a desirable goal, it may be more feasible to identify compounds that share the same biotransformation pathway in order to first develop (Q)SARs or expert guidance rules for the most relevant biotransformation processes. Given the importance of bio-

DOI: 10.1021/acs.est.6b03504
Environ. Sci. Technol. 2016, 50, 12722−12731

transformation as a mechanism for eliminating hydrophobic chemicals, the extension of the present data set to include more hydrophobic structures (e.g., longer alkyl chain lengths) may help define the relationship(s) between biotransformation rate and hydrophobicity and clarify the importance of other factors relating to molecular size and shape. As shown for C_{12}-2-LAS and pentachlorophenol in this study, the absence of significant or detectable biotransformation rates in the RT-S9 assay does not necessarily imply that the test chemical is resistant to biotransformation or that biotransformation rates are low. The RT-S9 results should be compared with results from other in vitro assay systems (i.e., hepatocytes) as well as in vivo data to better define possible limitations of the S9 method and perhaps in vitro methods in general. Comparative evaluations of methods for a broader range of chemicals may also provide guidance as to which in vitro systems are most appropriate for certain different chemical classes, functional groups, and metabolic pathways to help inform the development and application of integrated (tiered) testing strategies for assessing bioaccumulation potential.

■ ASSOCIATED CONTENT

Supporting Information

The Supporting Information is available free of charge on the ACS Publications website at DOI: 10.1021/acs.est.6b03504.

IOCs included in the in vivo k_B-QSAR training set, details of the RT-S9 assay, chemical properties and suppliers, consistency analysis, and raw depletion curves data (PDF)

■ AUTHOR INFORMATION

Corresponding Author

*Tel.: +31 20525 7439; e-mail: steven.droge@gmail.com.

Present Address

¶S.T.J.D.: UvA-IBED, Postbus 94248, 1090 GE Amsterdam, The Netherlands.

Notes

The authors declare no competing financial interest.

■ ACKNOWLEDGMENTS

This research was financially supported by the European Chemical Industry Council's Long-range Research Initiative program (Cefic-LRi) as part of the ECO21 project. The European Centre for Ecotoxicology and Toxicology of Chemicals (ECETOC) is acknowledged for managing the project, and discussions with various ECETOC monitoring team members were highly appreciated.

■ REFERENCES

(1) Manallack, D. T. The acid-base profile of a contemporary set of drugs: Implications for drug discovery. *SAR QSAR Environ. Res.* **2009**, *20*, 611−655.

(2) Rayne, S.; Forest, K. Dow and Kaw,eff vs. Kow and Kaw: Acid/base ionization effects on partitioning properties and screening commercial chemicals for long-range transport and bioaccumulation potential. *J. Environ. Sci. Health, Part A: Toxic/Hazard. Subst. Environ. Eng.* **2010**, *45*, 1550−1594.

(3) Franco, A.; Ferranti, A.; Davidsen, C.; Trapp, S. An unexpected challenge: Ionizable compounds in the REACH chemical space. *Int. J. Life Cycle Assess.* **2010**, *15*, 321−325.

(4) Charifson, P. S.; Walters, W. P. Acidic and basic drugs in medicinal chemistry: A perspective. *J. Med. Chem.* **2014**, *57*, 9701−9717.

(5) Lloyd, J. U. Scientific section discovery of the alkaloidal affinities of hydrous aluminum silicate. *J. Am. Pharm. Assoc.* **1916**, *5*, 381−390.

(6) Bailey, G. W.; White, J. L.; Rothberg, T. Adsorption of organic herbicides by montmorillonite: role of pH and chemical character of adsorbate. *Soil Sci. Soc. Am. Proc.* **1968**, *32*, 222−234.

(7) Zhang, Z. Z.; Sparks, D. L.; Scrivner, N. C. Sorption and desorption of quaternary amine cations on clays. *Environ. Sci. Technol.* **1993**, *27*, 1625−1631.

(8) MacManus-Spencer, L. A.; Tse, M. L.; Hebert, P. C.; Bischel, H. N.; Luthy, R. G. Binding of perfluorocarboxylates to serum albumin: a comparison of analytical methods. *Anal. Chem.* **2010**, *82*, 974−981.

(9) Jafvert, C. T.; Westall, J. C.; Grieder, E.; Schwarzenbach, R. P. Distribution of hydrophobic ionogenic organic compounds between octanol and water: organic acids. *Environ. Sci. Technol.* **1990**, *24*, 1795−1803.

(10) Escher, B. I.; Schwarzenbach, R. P. Partitioning of substituted phenols in liposome-water, biomembrane-water, and octanol-water systems. *Environ. Sci. Technol.* **1996**, *30*, 260−270.

(11) Bischel, H. N.; MacManus-Spencer, L. A.; Luthy, R. G. Noncovalent interactions of long-chain perfluoroalkyl acids with serum albumin. *Environ. Sci. Technol.* **2010**, *44*, 5263−5269.

(12) Armitage, J. M.; Arnot, J. A.; Wania, F. Potential role of phospholipids in determining the internal tissue distribution of perfluoroalkyl acids in biota. *Environ. Sci. Technol.* **2012**, *46*, 12285−12286.

(13) Ng, C. A.; Hungerbühler, K. Bioaccumulation of perfluorinated alkyl acids: Observations and models. *Environ. Sci. Technol.* **2014**, *48*, 4637−4648.

(14) Neuwoehner, J.; Escher, B. I. The pH-dependent toxicity of basic pharmaceuticals in the green algae *Scenedesmus vacuolatus* can be explained with a toxicokinetic ion-trapping model. *Aquat. Toxicol.* **2011**, *101*, 266−275.

(15) MacKay, A. A.; Vasudevan, D. Polyfunctional ionogenic compound sorption: challenges and new approaches to advance predictive models. *Environ. Sci. Technol.* **2012**, *46*, 9209−9223.

(16) Hyland, K. C.; Dickenson, E. R. V.; Drewes, J. E.; Higgins, C. P. Sorption of ionized and neutral emerging trace organic compounds onto activated sludge from different wastewater treatment configurations. *Water Res.* **2012**, *46*, 1958−1968.

(17) Chen, Y.; Hermens, J. L. M.; Droge, S. T. J. Influence of organic matter type and medium composition on the sorption affinity of C12-benzalkonium cation. *Environ. Pollut.* **2013**, *179*, 153−159.

(18) Droge, S. T. J.; Goss, K.-U. Effect of sodium and calcium cations on the ion-exchange affinity of organic cations for soil organic matter. *Environ. Sci. Technol.* **2012**, *46*, 5894−5901.

(19) Droge, S. T. J.; Goss, K.-U. Sorption of organic cations to phyllosilicate clay minerals: CEC-normalization, salt dependency, and the role of electrostatic and hydrophobic effects. *Environ. Sci. Technol.* **2013**, *47*, 14224−14232.

(20) Droge, S. T. J.; Goss, K.-U. Development and evaluation of a new sorption model for organic cations in soil: Contributions from organic matter and clay minerals. *Environ. Sci. Technol.* **2013**, *47*, 14233−14241.

(21) Miller, E. L.; Nason, S. L.; Karthikeyan, K. G.; Pedersen, J. A. Root uptake of pharmaceuticals and personal care product ingredients. *Environ. Sci. Technol.* **2016**, *50*, 525−541.

(22) Teeguarden, J. G.; Tan, Y. M.; Edwards, S.; Leonard, J. A.; Anderson, K. A.; Corley, R. A.; Kile, M.; Simonich, S. M.; Stone, D.; Tanguay, R. L.; Waters, K. M.; Harper, S.; Williams, D. E. Completing the link between exposure science and toxicology for improved environmental health decision making: The aggregate exposure pathway framework. *Environ. Sci. Technol.* **2016**, *50*, 4579−4586.

(23) Escher, B. I.; Ashauer, R.; Dyer, S. D.; Hermens, J. L. M.; Lee, J.-H.; Leslie, H. A.; Mayer, P.; Meador, J. P.; Warne, M. S. J. Crucial role of mechanisms and modes of toxic action for understanding tissue residue toxicity and internal effect concentrations of organic chemicals. *Integr. Environ. Assess. Manage.* **2011**, *7*, 28−49.

(24) Escher, B. I.; Hermens, J. L. M. Modes of action in ecotoxicology: Their role in body burdens, species sensitivity,

DOI: 10.1021/acs.est.6b03504
Environ. Sci. Technol. 2016, 50, 12722−12731

QSARs, and mixture effects. *Environ. Sci. Technol.* **2002**, *36*, 4201−4217.
(25) Armitage, J. M.; Arnot, J. A.; Wania, F.; Mackay, D. Development and evaluation of a mechanistic bioconcentration model for ionogenic organic chemicals in fish. *Environ. Toxicol. Chem.* **2013**, *32*, 115−128.
(26) Barber, M. C. A review and comparison of models for predicting dynamic chemical bioconcentration in fish. *Environ. Toxicol. Chem.* **2003**, *22*, 1963−1992.
(27) Gobas, F. A. P. C. A model for predicting the bioaccumulation of hydrophobic organic chemicals in aquatic food-webs: application to Lake Ontario. *Ecol. Modell.* **1993**, *69*, 1−17.
(28) Arnot, J. A.; Gobas, F. A. P. C. A food web bioaccumulation model for organic chemicals in aquatic ecosystems. *Environ. Toxicol. Chem.* **2004**, *23*, 2343−2355.
(29) Thomann, R. V. Bioaccumulation model of organic chemical distribution in aquatic food chains. *Environ. Sci. Technol.* **1989**, *23*, 699−707.
(30) De Wolf, W.; De Bruijn, J. H. M.; Seinen, W.; Hermens, J. L. M. Influence of biotransformation on the relationship between bioconcentration factors and octanol-water partition coefficients. *Environ. Sci. Technol.* **1992**, *26*, 1197−1201.
(31) Cowan-Ellsberry, C. E.; Dyer, S. D.; Erhardt, S.; Bernhard, M. J.; Roe, A. L.; Dowty, M. E.; Weisbrod, A. V. Approach for extrapolating in vitro metabolism data to refine bioconcentration factor estimates. *Chemosphere* **2008**, *70*, 1804−1817.
(32) Nichols, J. W.; Huggett, D. B.; Arnot, J. A.; Fitzsimmons, P. N.; Cowan-Ellsberry, C. E. Toward improved models for predicting bioconcentration of well-metabolized compounds by rainbow trout using measured rates of in vitro intrinsic clearance. *Environ. Toxicol. Chem.* **2013**, *32*, 1611−1622.
(33) Cravedi, J. P.; Lafuente, A.; Baradat, M.; Hillenweck, A.; Perdu-Durand, E. Biotransformation of pentachlorophenol, aniline and biphenyl in isolated rainbow trout (*Oncorhynchus mykiss*) hepatocytes: Comparison with in vivo metabolism. *Xenobiotica* **1999**, *29*, 499−509.
(34) Tolls, J.; Haller, M.; Sijm, D. T. H. M. Extraction and isolation of linear alkylbenzenesulfonate and its sulfophenylcarboxylic acid metabolites from fish samples. *Anal. Chem.* **1999**, *71*, 5242−5247.
(35) Tolls, J.; Lehmann, M. P.; Sijm, D. T. H. M. Quantification of in vivo biotransformation of the anionic surfactant C-12−2-linear alkylbenzene sulfonate in fathead minnows. *Environ. Toxicol. Chem.* **2000**, *19*, 2394−2400.
(36) Gomez, C. F.; Constantine, L.; Huggett, D. B. The influence of gill and liver metabolism on the predicted bioconcentration of three pharmaceuticals in fish. *Chemosphere* **2010**, *81*, 1189−1195.
(37) Gomez, C. F.; Constantine, L.; Moen, M.; Vaz, A.; Wang, W.; Huggett, D. B. Ibuprofen metabolism in the liver and gill of rainbow trout. *Bull. Environ. Contam. Toxicol.* **2011**, *86*, 247−251.
(38) Arnot, J. A.; Mackay, D.; Bonnell, M. Estimating metabolic biotransformation rates in fish from laboratory data. *Environ. Toxicol. Chem.* **2008**, *27*, 341−351.
(39) Arnot, J. A.; Mackay, D.; Parkerton, T. F.; Bonnell, M. A database of fish biotransformation rates for organic chemicals. *Environ. Toxicol. Chem.* **2008**, *27*, 2263−2270.
(40) Brown, T. N.; Arnot, J. A.; Wania, F. Iterative fragment selection: A group contribution approach to predicting fish biotransformation half-lives. *Environ. Sci. Technol.* **2012**, *46*, 8253−8260.
(41) Papa, E.; Van der Wal, L.; Arnot, J. A.; Gramatica, P. Metabolic biotransformation half-lives in fish: QSAR modeling and consensus analysis. *Sci. Total Environ.* **2014**, *470−471*, 1040−1046.
(42) Escher, B. I.; Cowan-Ellsberry, C. E.; Dyer, S. D.; Embry, M. R.; Erhardt, S.; Halder, M.; Kwon, J.-H.; Johanning, K.; Oosterwijk, M. T. T.; Rutishauser, S.; Segner, H.; Nichols, J. Protein and lipid binding parameters in rainbow trout (Oncorhynchus mykiss) blood and liver fractions to extrapolate from an in vitro metabolic degradation assay to in vivo bioaccumulation potential of hydrophobic organic chemicals. *Chem. Res. Toxicol.* **2011**, *24*, 1134−1143.
(43) Arnot, J. A.; Meylan, W.; Tunkel, J.; Howard, P. H.; Mackay, D.; Bonnell, M.; Boethling, R. S. A quantitative structure-activity relationship for predicting metabolic biotransformation rates for organic chemicals in fish. *Environ. Toxicol. Chem.* **2009**, *28*, 1168−1177.
(44) Gomez, C. F.; Constantine, L.; Huggett, D. B. The influence of gill and liver metabolism on the predicted bioconcentration of three pharmaceuticals in fish. *Chemosphere* **2010**, *81*, 1189−1195.
(45) Gröner, F.; Ziková, A.; Kloas, W. Effects of the pharmaceuticals diclofenac and metoprolol on gene expression levels of enzymes of biotransformation, excretion pathways and estrogenicity in primary hepatocytes of Nile tilapia (*Oreochromis niloticus*). *Comp. Biochem. Physiol., Part C: Toxicol. Pharmacol.* **2015**, *167*, 51−57.
(46) Mehinto, A. C.; Hill, E. M.; Tyler, C. R. Uptake and biological effects of environmentally relevant concentrations of the nonsteroidal anti-inflammatory pharmaceutical diclofenac in rainbow trout (*Oncorhynchus mykiss*). *Environ. Sci. Technol.* **2010**, *44*, 2176−2182.
(47) Connors, K. A.; Du, B.; Fitzsimmons, P. N.; Hoffman, A. D.; Chambliss, C. K.; Nichols, J. W.; Brooks, B. W. Comparative pharmaceutical metabolism by rainbow trout (*Oncorhynchus mykiss*) liver S9 fractions. *Environ. Toxicol. Chem.* **2013**, *32*, 1810−1818.
(48) Johanning, K.; Hancock, G.; Escher, B.; Adekola, A.; Bernhard, M.; Cowan-Ellsberry, C.; Domoradzki, J.; Dyer, S.; Eickhoff, C.; Embry, M.; Erhardt, S.; Fitzsimmons, P.; Halder, M.; Hill, J.; Holden, D.; Johnson, R.; Rutishauser, S.; Segner, H.; Schultz, I.; Nichols, J. Assessment of metabolic stability using the rainbow trout (*Oncorhynchus mykiss*) liver S9 fraction. *Curr. Protoc. Toxicol.* **2012**, *1*, 14−10.
(49) Houston, B. J. Utility of in vitro drug metabolism data in predicting in vivo metabolic clearance. *Biochem. Pharmacol.* **1994**, *47*, 1469−1479.
(50) Houston, B. J.; Carlile, D. J. Prediction of hepatic clearance from microsomes, hepatocytes, and liver slices. *Drug Metab. Rev.* **1997**, *29*, 891−922.
(51) Iwatsubo, T.; Hirota, N.; Ooie, T.; Suzuki, H.; Shimada, N.; Chiba, K.; et al. Prediction of in vivo drug metabolism in the human liver from in vitro metabolism data. *Pharmacol. Ther.* **1997**, *73*, 147−171.
(52) Obach, R. S.; Baxter, J. G.; Liston, T. E.; Silber, B. M.; Jones, B. C.; Macintyre, F.; Rance, D. J.; Wastall, P. The prediction of human pharmacokinetic parameters from preclinical and in vitro metabolism data. *J. Pharmacol. Exp. Ther.* **1997**, *283*, 46−58.
(53) Nichols, J. W.; Hoffman, A. D.; Ter Laak, T. L.; Fitzsimmons, P. N. Hepatic clearance of 6 polycyclic aromatic hydrocarbons by isolated perfused trout livers: Prediction from In vitro clearance by liver S9 fractions. *Toxicol. Sci.* **2013**, *136*, 359−372.
(54) Ladd, M. A.; Fitzsimmons, P. N.; Nichols, J. W. Optimization of a UDP-glucuronosyltransferase assay for trout liver S9 fractions: activity enhancement by alamethicin, a pore-forming peptide. *Xenobiotica* **2016**, *46*, 1066.
(55) Lintz, W.; Erlacin, S.; Frankus, E.; Uragg, H. Biotransformation of tramadol in man and animal. *Arzneim.-Forsch/Drug Res.* **1981**, *31*, 1932−1943.
(56) Paton, D. M.; Webster, D. R. Clinical pharmacokinetics of H1-receptor antagonists (the antihistamines). *Clin. Pharmacokinet.* **1985**, *10*, 477−497.
(57) Nałęcz-Jawecki, G. In vitro biotransformation of amitriptyline and imipramine with rat hepatic S9 fraction: Evaluation of the toxicity with spirotox and thamnotoxkit F tests. *Arch. Environ. Contam. Toxicol.* **2008**, *54*, 266−273.
(58) Nakamura, Y.; Yamamoto, H.; Sekizawa, J.; Kondo, T.; Hirai, N.; Tatarazako, N. The effects of pH on fluoxetine in Japanese medaka (*Oryzias latipes*): Acute toxicity in fish larvae and bioaccumulation in juvenile fish. *Chemosphere* **2008**, *70*, 865−873.
(59) Tarazona, J. V.; Escher, B. I.; Giltrow, E.; Sumpter, J.; Knacker, T. Targeting the environmental risk assessment of pharmaceuticals: Facts and fantasies. *Integr. Environ. Assess. Managem.* **2010**, *6*, 603−613.
(60) Droge, S. T. J.; Hermens, J. L. M.; Rabone, J.; Gutsell, S.; Hodges, G. Phospholipophilicity of $CxHyN^+$ amines: Chromato-

DOI: 10.1021/acs.est.6b03504
Environ. Sci. Technol. 2016, 50, 12722−12731

graphic descriptors and molecular simulations for understanding partitioning into membranes. *Environ. Sci.: Processes Impacts.* **2016**, *18*, 1011−1123.
(61) Nałęcz-Jawecki, G.; Wójcik, T.; Sawicki, J. Evaluation of in vitro biotransformation of propranolol with HPLC, MS/MS, and two bioassays. *Environ. Toxicol.* **2008**, *23*, 52−58.
(62) Mehvar, R.; Brocks, D. R. Stereospecific pharmacokinetics and pharmacodynamics of beta-adrenergic blockers in humans. *J. Pharm. Pharm. Sci.* **2001**, *4*, 185−200.
(63) Bussy, U.; Delaforge, M.; El-Bekkali, C.; Ferchaud-Roucher, V.; Krempf, M.; Tea, I.; Galland, N.; Jacquemin, D.; Boujtita, M. Acebutolol and alprenolol metabolism predictions: Comparative study of electrochemical and cytochrome P450-catalyzed reactions using liquid chromatography coupled to high-resolution mass spectrometry. *Anal. Bioanal. Chem.* **2013**, *405*, 6077−6085.
(64) Volotinen, M.; Korjamo, T.; Tolonen, A.; Turpeinen, M.; Pelkonen, O.; Hakkola, J.; et al. Effects of selective serotonin reuptake inhibitors on timolol metabolism in human liver microsomes and cryopreserved hepatocytes. *Basic Clin. Pharmacol. Toxicol.* **2010**, *106*, 302−309.
(65) Connors, K. A.; Du, B.; Fitzsimmons, P. N.; Chambliss, C. K.; Nichols, J. W.; Brooks, B. W. Enantiomer-specific in vitro biotransformation of select pharmaceuticals in rainbow trout (*Oncorhynchus mykiss*). *Chirality* **2013**, *25*, 763−767.
(66) Lo, J. C.; Allard, G. N.; Otton, S. V.; Campbell, D. A.; Gobas, F. A. P. C. Concentration dependence of biotransformation in fish liver S9: Optimizing substrate concentrations to estimate hepatic clearance for bioaccumulation assessment. *Environ. Toxicol. Chem.* **2015**, *34*, 2782−2790.
(67) Tolls, J. Bioconcentration of Surfactants. Ph.D. Dissertation, Utrecht University, Utrecht, 1998.
(68) Dyer, S. D.; Bernhard, M. J.; Cowan-Ellsberry, C.; Perdu-Durand, E.; Demmerle, S.; Cravedi, J. P. In vitro biotransformation of surfactants in fish. Part I: Linear alkylbenzene sulfonate (C12-LAS) and alcohol ethoxylate (C13EO8). *Chemosphere* **2008**, *72*, 850−862.

DOI: 10.1021/acs.est.6b03504
Environ. Sci. Technol. 2016, 50, 12722−12731